

On Block-Reference Coherent Diffraction Imaging

David Barmherzig, Ju Sun, Po-Nan Li, and T.J. Lane

Stanford University and SLAC National Accelerator Laboratory
 {davidbar,sunju,liponan}@stanford.edu, tjlane@slac.stanford.edu

Abstract: We show the advantage of the constant block-reference over alternatives for extended-reference CDI in terms of noise stability and physical feasibility.

OCIS codes: 70.0070, 100.5070

1. Extended-reference CDI

In coherent diffraction imaging (CDI), one observes, to good approximation, the oversampled Fourier magnitudes of the absorption density of a specimen. Recovering the density from the magnitudes leads to the classic phase retrieval problem. Recovery has traditionally been performed by iterative methods that combine the knowledge of a limited support (oversampling) in image space and Fourier magnitudes [1]. Such methods, however, are susceptible to failure due to imperfections commonly found in experimental data: noise, missing measurements, and background signals. Moreover, there is no guarantee these methods can solve the underlying nonconvex optimization problem for recovery. In real-world settings, obtaining a robust solution often necessitates many repeated reconstructions using multiple algorithms, parameters, and random restarts.

One way of countering these difficulties is adding a known reference specimen alongside the original, called extended-reference CDI [2, 3]. In this paper, we focus on a generic setup as illustrated in Fig. 1(a), where for simplicity we assume the reference R has the same size as the original specimen.

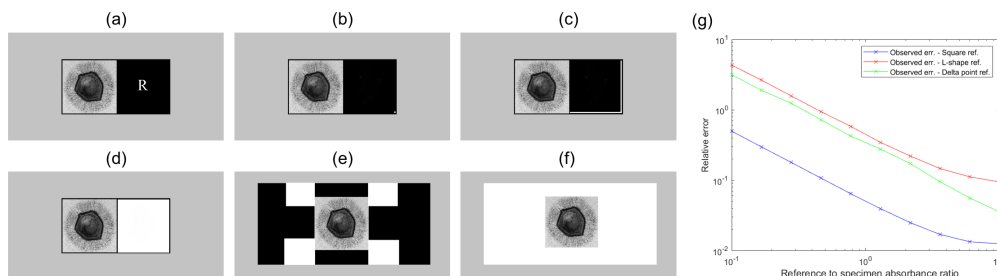


Fig. 1: Reference choices for extended-reference CDI and error comparison. (a): Generic setup. (b)–(d): Point-source/L-shaped/block-reference. (e)–(f): Variants of the block-reference scheme. (g): Relative shot (Poisson) noise error vs. absorbance ratio of reference to (mimivirus [4]) specimen for various reference schemes.

The case where R is a point-source (i.e. a delta function) (Fig. 1(b)) amounts to classic Fourier holography [5]. The L -shaped (Fig. 1(c)) and constant block (Fig. 1(d)) references were initially proposed in [3] and [2], respectively, among other possibilities [6, 7].

For recovery, reference-specific non-iterative methods have been derived [2, 3, 5]. Here we elucidate the simple and general mathematics behind these specific recovery schemes. Previously, stabilities of the different references have not been carefully evaluated. We provide both empirical and theoretical results, showing that the block-reference scheme achieves the best stability.

2. Recovery as (partial) deconvolution & Stability

Let $[X, R]$ be the extended specimen, where R is the known reference. Then, $\hat{Y} = \text{Pois}(|\mathcal{F}([X, R])|^2)$ is the observation (where $\text{Pois}(\lambda)$ denotes the Poisson distribution with rate λ , and \mathcal{F} denotes the oversampled Fourier transform). Here we explicitly model two sources of imperfections: \mathcal{F} could sample nonuniform points in the frequency domain, e.g. a beam stop that blocks low-frequency components, and the measurements are contaminated by shot (Poisson) noise.

We can obtain from \hat{Y} an estimate for the autocorrelation of $[X, R]$, $A_{[X,R]}$ by solving the least squares $\min_A \frac{1}{2} \|\hat{Y} - \mathcal{F}(A)\|_2^2$, which admits a unique closed-form solution $\hat{A}_{[X,R]}$ when \mathcal{F} contains enough frequency samples. We can then extract from $\hat{A}_{[X,R]}$ the part $\hat{C}_{[R,X]}$, an estimate for the first half of the cross-correlation $(R \star X)_H$, which is linear in X . Finally, an estimate for X is obtained by performing deconvolution on $\hat{C}_{[R,X]}$ based on the known R : $\min_X \frac{1}{2} \|\hat{C}_{[R,X]} - (R \star X)_H\|_2^2$ which gives $\hat{X} = M_R^{-1}(\hat{C}_{[R,X]})$, where M_R^{-1} is the inverse operator of the cross-correlation.

When R is L -shaped or a constant block, the differential operators proposed in [2, 3] have computable inverse operators and enable reconstruction in linear time with respect to the number of measured Fourier magnitudes. For a general reference shape, there may not a simple expression for the inverse operator. But it can be computed in quadratic time, instead of the usual cubic time, as the matrix M_R is always lower triangular.

When there is no shot noise, the above recovery method is exact. When noise is considered, we calculate the expected recovery error $\mathbb{E}\|\hat{X} - X\|_2^2$. Analysis shows the block reference scheme performs most favorably for signals with dominant low-frequency components, which is the case for generic specimens. This is supported by numerical simulations. In Fig. 1(g), we compare the relative reconstruction errors $\|\hat{X} - X\|_2 / \|X\|_2$ for the point-source, L -shaped, and constant block references across a range of reference-to-specimen absorbance ratios. The constant block scheme outperforms the other two by a significant margin.

3. Physical realization

We broadly define a block reference as any reference having a constant absorption density, and whose area incident to the imaging wavefront is equal to or greater than that of the specimen. Such a block reference can also be partially occluded by the specimen (see Fig. 1(e) and (f)). In addition to the recovery advantages discussed, a block reference also has the advantage that it does not require the fabrication of sharply varying internal features, as do the point-source and L -shaped references.

Modern lithography and nano-scale printing techniques mean the fabrication of block-referenced specimens is straightforward, if potentially expensive. For X-ray or electron imaging, single crystal silicon supports with thin silicon, silicon nitride or graphene backing have become popular as low-background substrates for fixed target imaging, such as the recent work by Seuring *et al.* [8]. These substrates exhibit windows etched into a single crystal silicon chip, which can be performed with high precision (order of 1 μm). We envision employing such chips, but further patterning a silicon block reference directly into the chip windows during etching, or printing a plastic or metallic square onto the windows post-fabrication. This technology has not yet been investigated in detail; costs associated with these fabrication tasks are still being researched. While the block-reference requires additional experimental complexity compared to reference free CDI, fabrication of extended rectangular references is simple compared to other reference shapes.

Acknowledgements

D.B. and J.S. wish to thank their research advisor Emmanuel J. Candès, and Walter Murray for helpful discussions.

References

1. S. Marchesini, "Invited article: A unified evaluation of iterative projection algorithms for phase retrieval," *Review of scientific instruments* **78**, 011,301 (2007).
2. S. Podorov, K. Pavlov, and D. Paganin, "A non-iterative reconstruction method for direct and unambiguous coherent diffractive imaging," *Optics express* **15**, 9954–9962 (2007).
3. M. Guizar-Sicairos and J. R. Fienup, "Holography with extended reference by autocorrelation linear differential operation," *Optics express* **15**, 17,592–17,612 (2007).
4. A. Levasseur *et al.*, "Mimivire is a defence system in mimivirus that confers resistance to virophone," *Nature* **531**, 249 (2016).
5. E. N. Leith and J. Upatnieks, "Reconstructed wavefronts and communication theory," *JOSA* **52**, 1123–1130 (1962).
6. M. Guizar-Sicairos and J. R. Fienup, "Direct image reconstruction from a fourier intensity pattern using heraldo," *Opt. Lett.* **33**, 2668–2670 (2008).
7. T. Gorkhover *et al.*, "Femtosecond x-ray fourier holography imaging of free-flying nanoparticles," *Nature Photonics* **12**, 150–153 (2018).
8. C. Seuring *et al.*, "Femtosecond x-ray coherent diffraction of aligned amyloid fibrils on low background graphene," *Nature communications* **9**, 1836 (2018).